Measurement of the Transverse Target and Beam-Target Asymmetries in η Meson Photoproduction at MAMI

C. S. Akondi,[1] J. R. M. Annand,[2] H. J. Arends,[3] R. Beck,[4] A. Bernstein,[5] N. Borisov,[6] A. Braghieri,[7] W. J. Briscoe,[8] S. Cherepnya,[9] C. Collicott,[10] S. Costanza,[7] E. J. Downie,[3,8] M. Dieterle,[11] A. Fix,[12] L. V. Fil'kov,[9] S. Garni,[11] D. I. Glazier,[13,2] W. Gradl,[3] G. Gurevich,[14] P. Hall Barrientos,[13] D. Hamilton,[2] D. Hornidge,[15] D. Howdle,[2] G. M. Huber,[16] V. L. Kashevarov,[3,9,*] I. Keshelashvili,[11] R. Kondratiev,[14] M. Korolija,[17] B. Krusche,[11] A. Lazarev,[6] V. Lisin,[14] K. Livingston,[2] I. J. D. MacGregor,[2] J. Mancel,[2] D. M. Manley,[1] P. Martel,[18,5] E. F. McNicoll,[2] W. Meyer,[19] D. Middleton,[15,3] R. Miskimen,[18] A. Mushkarenkov,[7,18] B. M. K. Nefkens,[20,†] A. Neganov,[6] A. Nikolaev,[4] M. Oberle,[11] M. Ostrick,[3,‡] H. Ortega,[3] P. Ott,[3] P. B. Otte,[3] B. Oussena,[3,8] P. Pedroni,[7] A. Polonski,[14] V. V. Polyanski,[9] S. Prakhov,[20] G. Reicherz,[19] T. Rostomyan,[11] A. Sarty,[10] S. Schumann,[3,5] O. Steffen,[3] I. I. Strakovsky,[8] Th. Strub,[11] I. Supek,[17] L. Tiator,[3] A. Thomas,[3] M. Unverzagt,[3] Yu. A. Usov,[6] D. P. Watts,[13] D. Werthmüller,[11] L. Witthauer,[11] and M. Wolfes[3]

(A2 Collaboration at MAMI)

[1]*Kent State University, Kent, Ohio 44242-0001, USA*
[2]*SUPA School of Physics and Astronomy, University of Glasgow, Glasgow G12 8QQ, United Kingdom*
[3]*Institut für Kernphysik, Johannes Gutenberg-Universität Mainz, D-55099 Mainz, Germany*
[4]*Helmholtz-Institut für Strahlen- und Kernphysik, University of Bonn, D-53115 Bonn, Germany*
[5]*Massachusetts Institute of Technology, Cambridge, Massachusetts 02139, USA*
[6]*Joint Institute for Nuclear Research, 141980 Dubna, Russia*
[7]*INFN Sezione di Pavia, I-27100 Pavia, Italy*
[8]*The George Washington University, Washington, DC 20052-0001, USA*
[9]*Lebedev Physical Institute, 119991 Moscow, Russia*
[10]*Department of Astronomy and Physics, Saint Marys University, Halifax, Nova Scotia B3H 3C3, Canada*
[11]*Departement für Physik, University of Basel, CH-4056 Basel, Switzerland*
[12]*Laboratory of Mathematical Physics, Tomsk Polytechnic University, 634034 Tomsk, Russia*
[13]*SUPA School of Physics, University of Edinburgh, Edinburgh EH9 3JZ, United Kingdom*
[14]*Institute for Nuclear Research, 125047 Moscow, Russia*
[15]*Mount Allison University, Sackville, New Brunswick E4L 1E6, Canada*
[16]*University of Regina, Regina, Saskatchewan S4S 0A2, Canada*
[17]*Rudjer Boskovic Institute, HR-10000 Zagreb, Croatia*
[18]*University of Massachusetts, Amherst, Massachusetts 01003, USA*
[19]*Institut für Experimentalphysik, Ruhr-Universität, D-44780 Bochum, Germany*
[20]*University of California Los Angeles, Los Angeles, California 90095-1547, USA*
(Received 12 June 2014; published 4 September 2014)

We present new data for the transverse target asymmetry T and the very first data for the beam-target asymmetry F in the $\vec{\gamma}\,\vec{p} \to \eta p$ reaction up to a center-of-mass energy of $W = 1.9$ GeV. The data were obtained with the Crystal-Ball/TAPS detector setup at the Glasgow tagged photon facility of the Mainz Microtron MAMI. All existing model predictions fail to reproduce the new data indicating a significant impact on our understanding of the underlying dynamics of η meson photoproduction. The peculiar nodal structure observed in existing T data close to threshold is not confirmed.

The electromagnetic production of η mesons is a selective probe to study resonance excitations of the nucleon ($N^\star$) for several reasons. First, because of the isoscalar nature of the η meson, $\Delta^\star$ excitations with isospin $I = 3/2$ do not contribute to the $\gamma N \to \eta N$ reactions. Second, because of the smallness of the ηNN coupling, nonresonant parts of the scattering amplitudes are strongly suppressed. Therefore, in contrast to the photoproduction of pions, the dynamics is dominated by resonance excitations. The

photoproduction of η mesons is part of the dedicated baryon resonance programs at MAMI, ELSA, and JLab and precision data on unpolarized cross sections and single-spin observables have already been obtained (see, e.g., Ref. [1] for a review). Preliminary results for double-spin observables from ELSA and JLab similar to the data presented in this Letter have been presented recently (see, e.g., Refs. [2,3]). Analyses of these data have been performed within single- and multichannel isobar models

[4–7] and coupled-channel approaches [8,9]. Furthermore, a partial-wave analysis has been performed within the SAID formalism [10]. All of these analyses agree in the fact that the low-energy behavior of the η production process is governed by the E_{0+} multipole amplitude, which is populated by the $N^\star(1535)1/2^-$ resonance. Higher mass $1/2^-$ resonances also appear to couple strongly to the ηN channel. Other resonances, with a small branching fraction to ηN, can be identified by exploiting the interference with the dominant E_{0+} amplitude in single- and double-spin observables. The beam asymmetry Σ, measured with a linearly polarized photon beam [11,12], and the transversely polarized target asymmetry T [13] are particularly sensitive to an interference of s-and d-wave amplitudes. A model independent analysis in the threshold region allowed for the determination of parameters of the $N^\star(1520)3/2^-$ resonance [14] and its contribution to η photoproduction. However, the target asymmetry data of Ref. [13] did not fit into this overall picture. The observed nodal structure in the threshold region could not be described by any reaction model using Breit-Wigner shapes for the parametrization of nucleon resonance contributions. The model independent, truncated multipole analysis [14] showed that this feature enforced a large and rapidly varying phase between the E_{0+} and the E_{2-}, M_{2-} multipoles. This phase was later supported by a measurement of the proton recoil polarization in the $p(e,e'\vec{p})\eta$ reaction [15]. However, such a strong phase motion is not possible between amplitudes dominated by two Breit-Wigner resonances with very close pole positions, the $N^\star(1535)1/2^-$ and the $N^\star(1520)3/2^-$ resonances. Since the original T data [13] had quite significant uncertainties, a more precise measurement of this observable in order to confirm or refute the nodal structure was highly desirable.

A second exciting observation was a narrow structure in the excitation function of η photoproduction off the neutron at $W = 1670$ MeV [16–19]. The position coincides with a dip observed in the $\gamma p \to \eta p$ total cross section [10]. The interpretations discussed in the literature include new narrow resonances, an interference between $1/2^-$ resonances, or coupled channel effects due to the opening of $K\Lambda$ and $K\Sigma$ channels.

In this Letter, we report a new, high-statistics measurement of η photoproduction from transversely polarized protons. The differential cross section is given by

$$\frac{d\sigma}{d\Omega} = \frac{d\sigma_0}{d\Omega}\left(1 + P_T \sin\phi\, T + h P_\odot P_T \cos\phi\, F\right). \quad (1)$$

Here $P_\odot$ and P_T denote the degree of circular beam and transverse target polarization, $h = \pm 1$ is the beam helicity, and ϕ is the azimuthal angle of the target polarization vector in a coordinate frame fixed to the reaction plane with $\hat{z} = \vec{p}_\gamma/|\vec{p}_\gamma|$, $\hat{y} = \vec{p}_\gamma \times \vec{p}_\eta/|\vec{p}_\gamma \times \vec{p}_\eta|$, and $\hat{x} = \hat{y} \times \hat{z}$.

The experiment was performed at the MAMI C accelerator in Mainz [20] using the Glasgow-Mainz tagged photon facility [21]. In the present measurement, a longitudinally polarized electron beam with an energy of 1557 MeV and a polarization degree of 80% was used. The tagged photon beam covers the energy range from 700 to 1450 MeV. The longitudinal polarization of electrons is transferred to circular polarization of the photons during the bremsstrahlung process in a radiator. The degree of circular polarization depends on the photon energy and ranged from 65% at 700 MeV to 78% at 1450 MeV [22]. The reaction $\gamma p \to \eta p$ was measured using the Crystal Ball (CB) [23] as the central spectrometer and TAPS [24] as a forward spectrometer. The combined CB/TAPS detection system covers 97% of the full solid angle. More details on the energy and angular resolution of the CB/TAPS detector system are given in Ref. [25].

The experiment requires transversely polarized protons, which were provided by a frozen-spin butanol (C_4H_9OH) target. A specially designed ^{3}He/^{4}He dilution refrigerator was built in order to maintain a temperature of 25 mK during the measurements. For transverse polarization, a four-layer saddle coil was installed as the holding magnet, which operated at a current of 35 A, corresponding to a field of 0.45 T. The target container, length 2 cm and diameter 2 cm, was filled with 2-mm diameter butanol spheres with a packing fraction (filling factor) of around 60%. The average proton polarization during the beam time periods May–June 2010 and April 2011 was 70% with relaxation times of around 1500 h. The target polarization was measured at the beginning and the end of each data taking period. In order to reduce the systematic errors, the direction of the target polarization vector was regularly reversed during the experiment. More details about the construction and operation of the target are given in Ref. [26].

The mesons were identified via the $\eta \to 2\gamma$ or $\eta \to 3\pi^0 \to 6\gamma$ decays. Selections on the 2γ, or 6γ, invariant mass distributions and on the missing mass $MM(\gamma p, \eta)$, calculated from the initial state and the reconstructed η meson, allowed for a clean identification of the reaction. In principle, the observables T and F in Eq. (1) can be determined in each energy and angular bin as count rate asymmetries from the number $N^\pm$ of reconstructed $\vec{\gamma}\,\vec{p} \to \eta p$ events with different orientations of target spin and beam helicity,

$$T = \frac{1}{P_T |\sin\phi|}\frac{N^{\pi=+1} - N^{\pi=-1}}{N^{\pi=+1} + N^{\pi=-1}}, \quad (2)$$

$$F = \frac{1}{P_T |\cos\phi|}\frac{1}{P_\odot}\frac{N^{\sigma=+1} - N^{\sigma=-1}}{N^{\sigma=+1} + N^{\sigma=-1}}, \quad (3)$$

where $\pi = \vec{p}_T \cdot \hat{y}/|\vec{p}_T \cdot \hat{y}| = \pm 1$ denotes the orientation of the target polarization vector $\vec{p}_T$ relative to the normal of the production plane and, in the case of the F asymmetry, $\sigma = h\vec{p}_T \cdot \hat{x}/|\vec{p}_T \cdot \hat{x}| = \pm 1$ is given by the product of the beam helicity h and the orientation of $\vec{p}_T$ relative to

the $\hat{x}$ axis. In these asymmetries, systematic uncertainties related to the reconstruction efficiency, the total photon flux normalization, and the target filling factor cancel. However, using butanol as the target material has an essential consequence because of the background coming from quasifree reactions on ^{12}C and ^{16}O nuclei. In the numerator of Eqs. (2) and (3), this background cancels because the nucleons bound in ^{12}C or ^{16}O are unpolarized. However, in order to determine the denominator, this contribution has to be taken into account. The detection of recoil protons and the requirement of coplanarity of the incoming photon and the outgoing hadrons already suppress this background significantly. The residual background has to be subtracted. In order to do this, the shape of the missing mass distribution $MM(\gamma p, \eta)$ was determined for η photoproduction on a pure carbon and a liquid hydrogen target. These templates were then fitted to the butanol data. Since the magnitude and the shape of the background depend on the initial beam energy and momenta of the final particles, the background subtraction procedure was performed for each energy and angular bin. This procedure is illustrated in Fig. 1 for two different examples at low and at high photon energy. Missing mass spectra for the reaction $\gamma p \rightarrow \eta p$ with the butanol target are shown in Figs. 1(a) and 1(b) by the black stars. Spectra measured with the hydrogen and carbon targets are presented on the same plots by the green triangles and the blue squares, correspondingly. Their absolute values were fitted to the butanol data with a typical reduced χ^2 between 0.7 and 1.5. The red circles, representing the sum of the hydrogen and carbon contribution, are the result of this fit. The signal is located around $MM(\gamma p, \eta) = m_p$. At higher missing masses and higher photon energies additional background from multimeson final states is observed. The number of signal events was determined in the regions between the vertical solid lines,
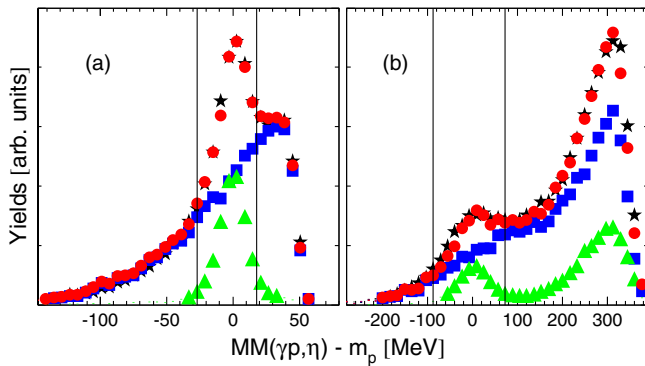

FIG. 1 (color online). Two typical examples of the carbon background subtraction, corresponding to an η meson polar angle around 90° and photon beam energies of 785 MeV (a) and 1350 MeV (b). The $MM(\gamma p, \eta)$ missing mass distributions obtained with butanol are shown as black stars. The green triangles and blue squares are the distributions obtained with hydrogen and carbon targets scaled to fit the butanol data. The red circles are the sum of the blue and green distributions.
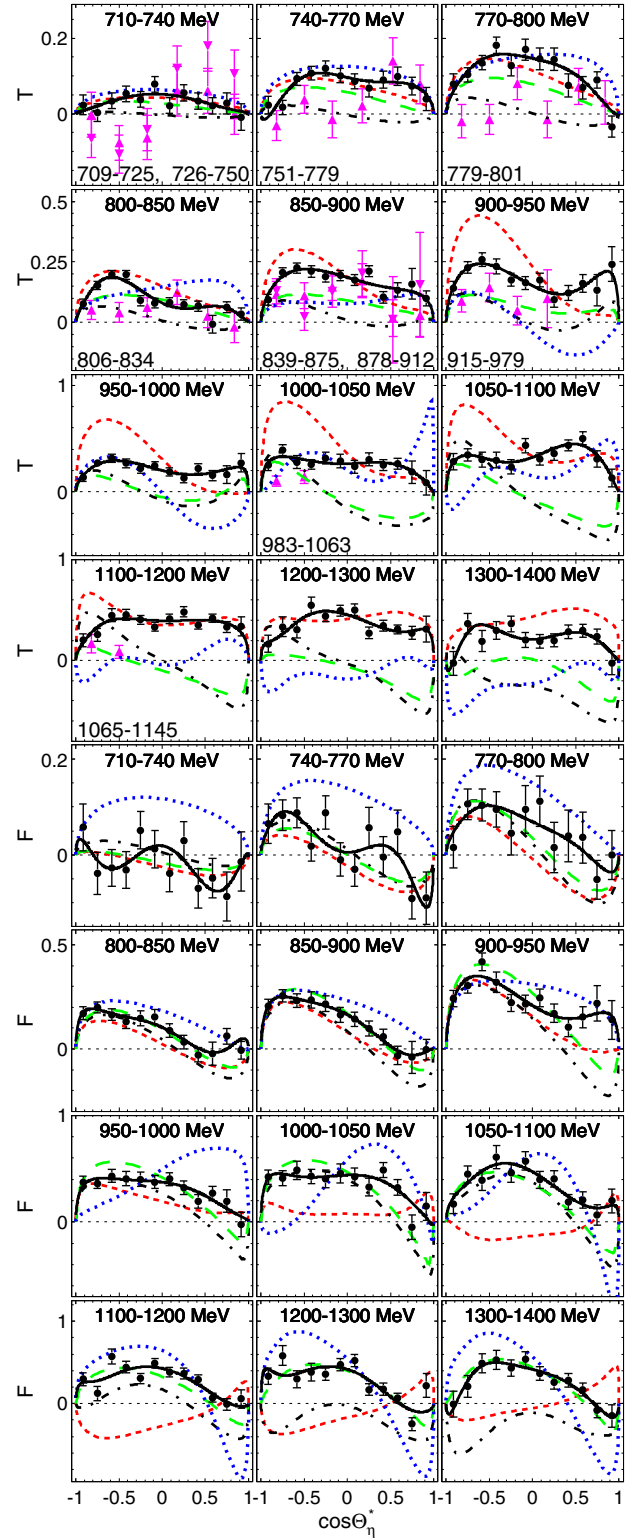

FIG. 2 (color online). T and F asymmetries. The new results with statistical uncertainties (black circles) are compared to existing data from Bonn [13] (magenta triangles) and existing partial-wave analysis predictions (red dashed: η-MAID [4], green long dashed: Giessen model [8], black dashed dotted: BG2011-02 [7], blue dotted: SAID GE09 [10]). The result of our Legendre fit is shown by the black curves, Eq. (3). The energy labels on the top of each panel indicate the photon energy bins for our data. The values at the bottom give the corresponding bins of Ref. [13].
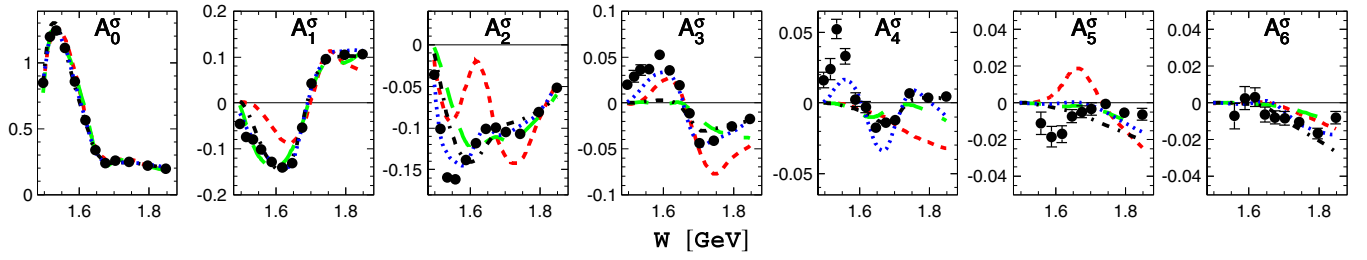
FIG. 3 (color online).   Legendre coefficients in [μb/sr] up to $\ell_{max} = 3$ from our fits to the differential cross section [10] as function of the center-of-mass energy W. Notations for the curves are the same as in Fig. 2.

which were selected to optimize the signal-to-background ratio and to remove background from multimeson production off polarized protons.

The systematic uncertainty is dominated by the determination of the degree of proton polarization (4%), the degree of photon beam polarization (2%), and the background subtraction procedure (3%–4%). By adding all contributions in quadrature, a total systematic uncertainty of less than 6% is obtained.

Figure 2 shows our results for T and F asymmetries together with previous data for T [13] and various theoretical predictions [4,6,8,10] for different bins in the incoming photon energy as a function of the η meson polar angle in the center-of-mass system, θ_η^*. The main inconsistencies with the existing data [13] are in the near threshold region. Here, our results do not confirm the observed nodal structure in the angular dependence of the T asymmetry and solve the long-standing question related to the relative phase between s- and d-wave amplitudes. Our data do not require any additional phase shift beyond a Breit-Wigner parametrization of resonances. This important conclusion is corroborated by preliminary data from ELSA [2]. At higher energies, all existing theoretical predictions of both T and F are in poor agreement among

themselves and with our experimental data, even though they describe the unpolarized differential cross sections well. The new data will therefore have a significant impact on the partial-wave structure of all models.

Furthermore, we present a fit of our cross section data [10] and the new polarization measurements based on an expansion in terms of Legendre polynomials truncated to a maximum orbital angular momentum ℓ_{max},

$$\frac{d\sigma}{d\Omega} = \sum_{n=0}^{2\ell_{max}} A_n^\sigma P_n(\cos\Theta_\eta), \tag{4}$$

$$T(F)\frac{d\sigma}{d\Omega} = \sin\Theta_\eta \sum_{n=0}^{2\ell_{max}-1} A_n^{T(F)} P_n(\cos\Theta_\eta). \tag{5}$$

The spin-dependent cross sections $Td\sigma/d\Omega$ and $Fd\sigma/d\Omega$ were obtained by multiplying the measured asymmetries with our results for the differential cross sections [10].

The results for the Legendre coefficients are presented in Figs. 3 and 4 together with the corresponding model calculations. For the differential cross section a truncation to $\ell_{max} = 2$ (d waves, A_4^σ) is sufficient below
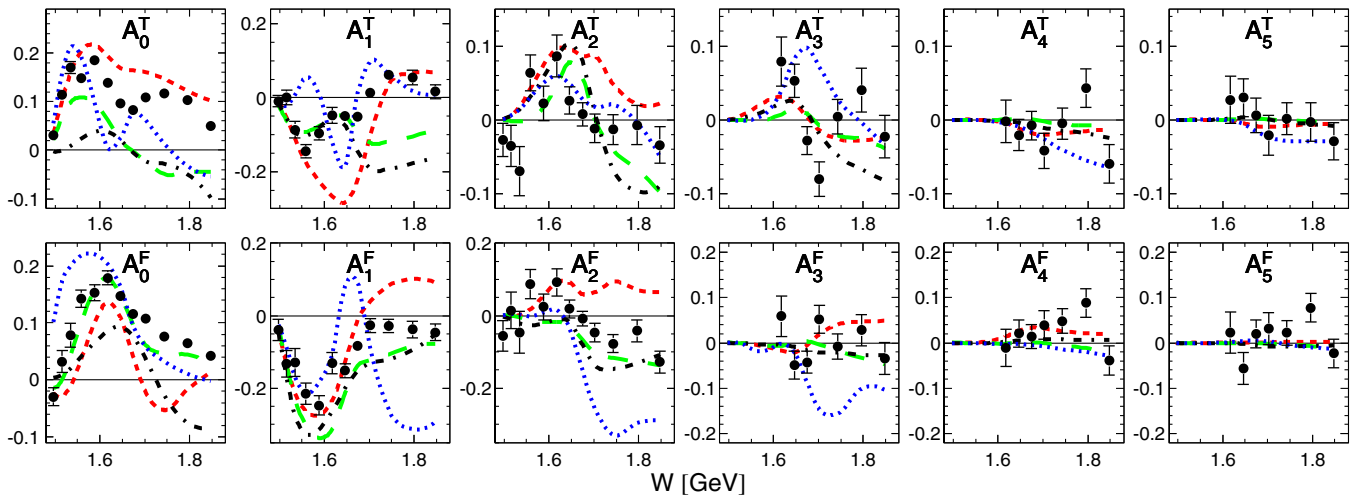

FIG. 4 (color online).   Legendre coefficients [μb/sr] up to $\ell_{max} = 3$ from our fits to the product of the new asymmetries with the differential cross section from Ref. [10]: $Td\sigma/d\Omega$ (upper row) and $Fd\sigma/d\Omega$ (lower row). Notations for the curves are the same as in Fig. 2.

$W = 1.6$ GeV and to $\ell_{\max} = 3$ (f waves, A_6^σ) above $W = 1.6$ GeV. Additional higher order terms do not improve the quality of the fit. For the new spin-dependent cross sections a truncation to pd interferences ($A_2^{T/F}$) below $W = 1.6$ GeV and df interferences ($A_4^{T/F}$) above $W = 1.6$ GeV is sufficient. The result of the Legendre fits is demonstrated in Fig. 2 by the black solid line. The models [7,8,10] that have been fitted to the differential cross section from Ref. [10] are, as expected, also in agreement with the coefficients in Fig. 3. Some deviations can be observed in A_5^σ, which is dominated by an interference between d and f waves. Despite this agreement, the corresponding predictions for the coefficients A_n^T and A_n^F do not agree with our results for all values of n even at low energies. The impact of the new data is therefore not restricted to a single partial-wave amplitude but is that all s-, p-, and d-wave amplitudes will be affected in future partial-wave analyses. This is in particular the case in the energy region around $W = 1670$ MeV, where the narrow structure in η production off neutrons is observed. A recent analysis in the framework of the Bonn-Gatchina analysis claimed that the structure can be completely explained by an interference of the $N^\star(1535)1/2^-$ and $N^\star(1650)1/2^-$ resonances without adding additional contributions from narrow states [27]. The Giessen model [8] also explains the structure by an interference within the E_{0+} partial wave. Here, the nature of the interference is related to coupled channel effects due to the opening of K-hyperon channels. However, as shown in Fig. 2, the predictions of both models for the target asymmetry in this energy region disagree completely with the new data, in shape as well as in sign. Consequently, such interpretations must be still taken with care and it has to be seen whether it is possible to refit these models including the new T data.

In summary, we have presented new experimental results for the target asymmetry T and the very first data on the transverse beam-target observable F for the $\vec{\gamma}\,\vec{p} \to \eta p$ reaction. The data solve a long-standing problem related to the angular dependence of older T data close to threshold. The unexpected relative phase motion between s- and d-wave amplitudes required by the old data is not confirmed. A Legendre decomposition of the new results shows the sensitivity to small partial-wave contributions. There is no evidence for any narrow structure. However, all existing solutions from various partial-wave analyses fail to reproduce the new data. We therefore expect a significant impact on future analyses and on our understanding of the dynamics of η photoproduction.

* kashev@kph.uni-mainz.de
† Deceased.
‡ ostrick@kph.uni-mainz.de

[1] V. Crede and W. Roberts, Rep. Prog. Phys. **76**, 076301 (2013).
[2] J. Hartmann, Proc. Sci., Hadron2013 (2013) 114, arXiv:1401.5998.
[3] B. G. Ritchie, EPJ Web Conf. **73**, 04010 (2014).
[4] W.-T. Chiang, S. N. Yang, L. Tiator, and D. Drechsel, Nucl. Phys. **A700**, 429 (2002).
[5] W.-T. Chiang, S. N. Yang, L. Tiator, M. Vanderhaeghen, and D. Drechsel, Phys. Rev. C **68**, 045202 (2003).
[6] A. V. Anisovich, E. Klempt, V. A. Nikonov, A. V. Sarantsev, and U. Thoma, Eur. Phys. J. A **47**, 27 (2011).
[7] A. V. Anisovich, E. Klempt, V. A. Nikonov, A. V. Sarantsev, and U. Thoma, Eur. Phys. J. A **47**, 153 (2011); A. V. Anisovich, R. Beck, E. Klempt, V. A. Nikonov, A. V. Sarantsev, and U. Thoma, Eur. Phys. J. A **48**, 15 (2012).
[8] V. Shklyar, H. Lenske, and U. Mosel, Phys. Rev. C **87**, 015201 (2013).
[9] H. Kamano, S. X. Nakamura, T.-S. H. Lee, and T. Sato, Phys. Rev. C **88**, 035209 (2013).
[10] E. F. McNicoll et al., Phys. Rev. C **82**, 035208 (2010).
[11] J. Ajaka et al., Phys. Rev. Lett. **81**, 1797 (1998).
[12] J. Elsner et al., Eur. Phys. J. A **33**, 147 (2007).
[13] A. Bock et al., Phys. Rev. Lett. **81**, 534 (1998).
[14] L. Tiator, D. Drechsel, G. Knochlein, and C. Bennhold, Phys. Rev. C **60**, 035210 (1999).
[15] H. Merkel et al., Phys. Rev. Lett. **99**, 132301 (2007).
[16] V. Kuznetsov et al., Phys. Lett. B **647**, 23 (2007).
[17] F. Miyahara et al., Prog. Theor. Phys. Suppl. **168**, 90 (2007).
[18] I. Jaegle et al., Phys. Rev. Lett. **100**, 252002 (2008); Eur. Phys. J. A **47**, 89 (2011).
[19] D. Werthmuller et al., Phys. Rev. Lett. **111**, 232001 (2013); L. Witthauer et al., Eur. Phys. J. A **49**, 154 (2013).
[20] K.-H. Kaiser et al., Nucl. Instrum. Methods Phys. Res., Sect. A **593**, 159 (2008).
[21] J. C. McGeorge et al., Eur. Phys. J. A **37**, 129 (2008); I. Anthony, J. D. Kellie, S. J. Hall, G. J. Miller, and J. Ahrens, Nucl. Instrum. Methods Phys. Res., Sect. A **301**, 230 (1991); S. J. Hall, G. J. Miller, R. Beck, and P. Jennewein, Nucl. Instrum. Methods Phys. Res., Sect. A **368**, 698 (1996).
[22] H. Olsen and L. C. Maximon, Phys. Rev. **114**, 887 (1959).
[23] A. Starostin et al., Phys. Rev. C **64**, 055205 (2001).
[24] R. Novotny, IEEE Trans. Nucl. Sci. **38**, 379 (1991); A. R. Gabler et al., Nucl. Instrum. Methods Phys. Res., Sect. A **346**, 168 (1994).
[25] S. Prakhov et al., Phys. Rev. C **79**, 035204 (2009); V. L. Kashevarov et al., Eur. Phys. J. A **42**, 141 (2009).
[26] A. Thomas, Eur. Phys. J. Spec. Top. **198**, 171 (2011).
[27] A. V. Anisovich, E. Klempt, V. A. Nikonov, A. V. Sarantsev, and U. Thoma, arXiv:1402.7164.